



The Magnetic Nature of the Cataclysmic Variable Period Gap

C. Garraffo^{1,2}, J. J. Drake¹, J. D. Alvarado-Gomez¹, S. P. Moschou¹, and O. Cohen³

¹Harvard-Smithsonian Center for Astrophysics, 60 Garden Street, Cambridge, MA 02138, USA; cgaraffo@cfa.harvard.edu

²Institute for Applied Computational Science, Harvard University, Cambridge, MA 02138, USA

³Lowell Center for Space Science and Technology, University of Massachusetts, Lowell, MA 01854, USA

Received 2018 August 28; revised 2018 September 28; accepted 2018 September 29; published 2018 November 20

Abstract

One of the most important problems in the context of cataclysmic variables (CVs) is the lack of observations of systems with periods between 2 and 3.12 hr, known as the period gap. The orbital evolution of CVs with periods shorter than those in the gap is dominated by gravitational radiation, while for periods exceeding those of the gap it is dominated by magnetic braking of the secondary star. Spruit & Ritter showed that as periods approach 3 hr and secondary stars become fully convective a sharp decline in magnetic dynamo and braking efficiency would result in such a gap. Recent X-ray observations finding coronal magnetic energy dissipation is similar in fully convective and partly radiative M dwarfs cast this theory into doubt. In this work, we use Zeeman–Doppler imaging observations culled from the literature to show that the complexity of the surface magnetic fields of rapidly rotating M dwarfs increases with decreasing rotation period. Garraffo et al. have shown that the efficiency of angular momentum loss of cool stars declines strongly with increasing complexity of their surface magnetic field. We explore the idea of Taam & Spruit that magnetic complexity might then explain the period gap. By generating synthetic CV populations using a schematic CV evolutionary approach, we show that the CV period gap can naturally arise as a consequence of a rise in secondary star magnetic complexity near the long-period edge of the gap that renders a sharp decline in their angular-momentum-loss rate.

Key words: binaries: close – stars: activity – stars: late-type – stars: rotation

1. Introduction

One of the most challenging puzzles in stellar evolution that emerged in the 1970s and early 1980s was the *cataclysmic variable period gap*. Cataclysmic variables (CVs) are interacting binary stars comprising a white dwarf accreting from either a main-sequence or slightly evolved star, or from a brown dwarf. As the population of known CVs grew, it became clear that systems with periods between 2 and 3.12 hr were rarely observed compared with objects with shorter and longer periods (Livio & Shaviv 1983; Ritter 1984; Knigge et al. 2011). While some of the underlying physics giving rise to this period gap are still debated, current models invoke changing rates of angular momentum loss as secondary stars are whittled down to lower and lower masses by attritional accretion onto their compact companion.

The orbital evolution of CVs with periods shorter than those in the gap is dominated by gravitational radiation (Faulkner 1971; Paczynski & Sienkiewicz 1981), while for periods exceeding those of the gap it is dominated by magnetic braking (Eggleton et al. 1976; Verbunt & Zwaan 1981). In the latter regime, systems lose angular momentum via the magnetized winds of the nondegenerate companion and, as a consequence, their orbital separation is reduced and they spin up. With mass from the secondary star being lost to the primary, the secondary star drifts to a later and later spectral type. By the time the system reaches the upper boundary of the period gap (~ 3.12 hr), the secondary star has been reduced to the mass of a fully convective M dwarf (Robinson et al. 1981; Spruit & Ritter 1983 and references therein).

Spruit & Ritter (1983) and Rappaport et al. (1983) showed that a fast decrease in angular momentum loss of $\sim 90\%$ as the secondary approaches the fully convective limit would result in strong suppression of the mass accretion from the secondary star onto its companion that would explain the appearance of

the period gap. A detailed review of this evolutionary scenario has been provided by Knigge et al. (2011). Typically, CVs are discovered through UV or X-ray emission from heated accreting material: if the accretion stops, the systems cannot be easily discerned.

The underlying motivation for a fairly abrupt angular-momentum-loss reduction at the fully convective limit stems from arguments that magnetic dynamo action in Sun-like stars occurs at the interface between the convection zone and the radiative interior—the “tachocline” (see, e.g., Spruit & Ritter 1983). The fact that the secondary star becomes fully convective near the edge of the period gap led to the idea that there is a fundamental change in the effectiveness of the dynamo at this limit. This supposed demise of the dynamo thus results in a magnetic braking “disruption.” However, evidence for such a dynamo demise has historically been weak or lacking. Recently, Wright & Drake (2016) have found that the X-ray emission level as a function of stellar rotation period is essentially the same for both fully convective and partly convective (more Sun-like) stars, including both rapid and slow rotators. X-ray activity has been shown to be a good proxy for surface magnetic flux (e.g., Pevtsov et al. 2003). Wright & Drake (2016) then argued that the invariance of X-ray behavior regardless of the presence or absence of a radiative zone supports the argument advanced by Spruit (2011) that magnetic dynamo action is instead distributed in the convection zone. The collateral effect of the Wright & Drake (2016) results is that, at face value, there is no change in the surface magnetic activity that drives magnetic braking: the *disrupted magnetic braking* theory for the CV period gap is broken. Taam & Spruit (1989) had anticipated this and suggested that the magnetic field of the secondary star might grow in complexity at the edge of the period gap, reducing the number of open field lines and the subsequent angular momentum loss.

Recently, it has been shown using different types of magnetohydrodynamic (MHD) wind models that the efficiency of angular momentum loss of cool stars strongly depends on the complexity of their stellar surface magnetic fields (Garraffo et al. 2015, 2016, hereafter CG16; Réville et al. 2015), echoing the earlier analytical conclusions of Taam & Spruit (1989). Garraffo et al. (2018, hereafter CG18) provided a new predictive spin-down model based on sophisticated MHD wind modeling that accounts for this magnetic modulation, and assumes that the complexity of the magnetic field is a function of Rossby number Ro ($Ro = P_{\text{rot}}/\tau$, where τ is convective turnover time). This assumption is well supported by Zeeman–Doppler imaging (ZDI) observations of the magnetic fields on the surfaces of Sun-like stars showing that faster rotating stars store a larger fraction of their magnetic flux in higher-order multipole components of the field (e.g., Donati 2003; Donati & Landstreet 2009; Marsden et al. 2011; Waite et al. 2011, 2015). As a consequence, they lose angular momentum much less efficiently.

Magnetic braking of CVs is usually modeled considering the secondary star as a single star and assuming it has a simple, fixed magnetic configuration such as a dipole. In this work, we study the available ZDI observations of late M dwarfs by Morin et al. (2010) to infer the underlying geometry of their magnetic fields as a function of rotation period. We follow the idea of Taam & Spruit (1989) and explore the possibility that there is an disruption of angular momentum loss near the upper boundary of the period gap (~ 3.12) resulting from an increasing magnetic complexity of the secondary star. Using the observed magnetic geometry of M dwarfs as a function of rotation period derived here and the spin-down model provided in CG18, we use the schematic method of Spruit & Ritter (1983) to reconstruct the orbital evolution of CVs near the gap period. Using this evolutionary recipe and the expected formation rate of CVs, we generate synthetic populations and predict the fraction of systems and their visibility as a function of orbital period.

The paper is organized as follows. In Section 2, we compute the complexity of the available ZDI observations for late M dwarfs and compare our data to the complexity function assumed in CG18. In Section 3, we use that function and the prescription for angular momentum loss from CG18 to describe a single system’s orbital evolution. In Section 4, we generate and evolve synthetic populations and compare them with observations. In Section 5, we discuss our findings and summarize our main conclusions.

2. Late M Dwarf Magnetic Complexity

The ZDI technique enables inference of the large-scale magnetic morphology of active cool stars fairly robustly given that the phase coverage of the observations is complete enough, or sufficiently high signal-to-noise ratios are achieved in poorly sampled data sets (Donati & Brown 1997; Hussain et al. 2000; Alvarado-Gómez et al. 2015). There is growing evidence from ZDI observations that faster rotating Sun-like stars show a more complex magnetic morphology on their surface (e.g., Donati 2003; Donati & Landstreet 2009; Marsden et al. 2011; Alvarado-Gómez et al. 2015; Waite et al. 2015). The importance of these observations lies in the results of MHD models of solar-like stellar winds that confirm the idea of Taam & Spruit (1989) and predict that an increase in the complexity of the magnetic fields should lead to a strong suppression of angular momentum loss

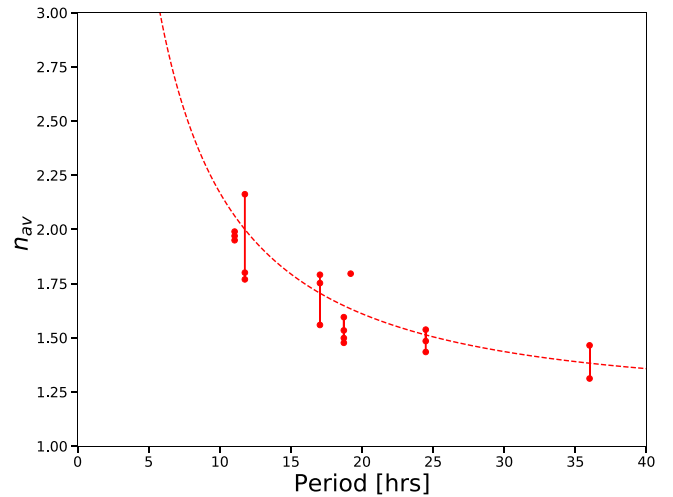


Figure 1. Magnetic complexity of available late M dwarf ZDI observations (dots) and the complexity function relating complexity, n_{av} , and rotation period from CG18 for a convective turnover time of $\tau_c = 100$ days (dashed curve). The connected dots represent different ZDI observations of the same star.

efficiency (Réville et al. 2015; Garraffo et al. 2015). It was shown by Garraffo et al. (2013, 2015) that only the first few terms ($Y_n^m(\theta, \psi) = N e^{im\psi} P_n^m(\cos \theta)$, $n \lesssim 7$) in a spherical harmonics decomposition of the surface field are relevant to this effect. At the same time, those first moments are the ones for which the ZDI technique is most reliable. We examine this here for late M dwarfs and study how it affects their rotational evolution.

We compute the large-scale magnetic complexity for all 19 available radial magnetic maps⁴ for the seven late M dwarfs (M5–M8) observed by Morin et al. (2010) following the spherical harmonic decomposition method of Garraffo et al. (2016). In this approach, the representative average complexity, n_{av} , is given by

$$n_{\text{av}} = \sum_{n=0}^{n_{\text{max}}} \frac{n F_n}{F_T}, \quad (1)$$

where F_n is the magnetic flux in each n -order term in the spherical harmonic decomposition and F_T is the total flux in the original magnetogram. CG16 and Finley et al. (2018) showed that angular-momentum-loss rates are independent of the different azimuthal distributions of magnetic flux (m modes) for a given complexity (n mode). It is on this basis that we neglect the parameter m in the decomposition. The results of application of Equation (1) for the Morin et al. (2010) late M dwarfs are plotted as a function of stellar rotation period in Figure 1. The ZDI maps show a trend of increasing complexity of the surface magnetic field for faster rotating stars that becomes more pronounced at the shortest periods of a few hours.

We compare the complexity derived from the observations to the magnetic complexity function in CG18, $n = \frac{a}{Ro} + Ro + 1$, in Figure 1. Here, Ro is the commonly used Rossby number for stellar magnetic dynamo activity representing the ratio $Ro = \tau_c/P_{\text{rot}}$ of rotation period, P_{rot} , and convective turnover time, τ_c . This complexity function was derived by matching the

⁴ GJ 51 (2006, 2007, and 2008), GJ 1156 (2007, 2008, and 2009), GJ 1245 (2006, 2007, and 2008), WX UMa (2006, 2007, 2008, and 2009), DX Cnc (2007, 2008, and 2009), GJ 3622 (2008, 2009), VB 10 (2009).

evolution of rotation periods of stars in young open clusters using the relationship between magnetic complexity and angular momentum loss derived by CG16.

The function shown in Figure 1 that provides a good match to the data corresponds to a convective turnover time $\tau_c = 100$ and value $a = 0.005$. The former is appropriate for the spectral types of the secondary stars considered here (Morin et al. 2010; Wright et al. 2011). The value of a is four times smaller than the one used by CG18, though we note that this quantity only affects the most rapidly rotating stars with the smallest Rossby numbers and was not well constrained in that study that only dealt with stars with masses greater than $0.3 M_\odot$. In our CV orbital evolution model (Section 3), we adopt an intermediate value $a = 0.01$. The shape of the complexity function, n , which dictates the change in angular momentum loss with changing rotation period, remains the same. It should also be kept in mind that, while n_{av} was shown to work reasonably well for parameterizing real magnetograms (Garraffo et al. 2016), there is some arbitrariness in its definition and it should strictly be interpreted only as a relative measure of complexity. The spatial resolution of ZDI-reconstructed magnetic fields is also limited by the rotation-induced velocity shift of surface magnetic features and the deconstructed complexity is inevitably going to be a lower limit to the true complexity.

3. Magnetic Disruption of Angular Momentum Loss

3.1. Angular Momentum Loss

Here, we simulate the orbital evolution of CVs, including, for the first time, the magnetic complexity modulation and its effect on angular momentum loss. We use the same spin-down model as presented by CG18.

As systems evolve and lose angular momentum, the orbits shrink and periods decrease. Efficient spin-orbit coupling means that the secondary stars spin up, maintaining synchronicity between their rotation and orbital periods. Figure 1 indicates that their magnetic complexity will also increase as they spin up. The data show a somewhat steeper increase in complexity for the stars with the shortest rotation periods, although data are lacking for periods less than 10 hr. We proceed by adopting the CG18 spin-down model and complexity function, taking Figure 1 as offering some empirical support (with the function reproducing well the data on average), but recognizing that it still represents somewhat of an extrapolation to reach the CV period gap. The spin-down model can then be described by the following equations (see CG18 for further details):

$$\dot{J} = \dot{J}_{\text{Dip}} Q_J(n_{\text{av}}), \quad (2)$$

$$Q_J(n_{\text{av}}) = 4.05 e^{-1.4n_{\text{av}}} + (n_{\text{av}} - 1)/(60B n_{\text{av}}), \quad (3)$$

where \dot{J} represents the angular-momentum-loss rate, \dot{J}_{Dip} the rate for a dipolar magnetic configuration. The factor $Q_J(n_{\text{av}})$ includes the magnetic morphology dependence, B stands for surface field strength [Gauss], and n stands for the magnetic multipolar moment describing the complexity of the field. As in CG18, we neglect the second term in Equation (3) because it is negligible for $n_{\text{av}} < 7$, which is the regime we are exploring here. As noted in Section 2, we adopt a value $a = 0.01$, which gives $\dot{J}/J_{\text{orb}} \approx 1 \times 10^{-8}$ for a period of 5 hr and $\approx 2. \times 10^{-9}$ just above the gap at 3.2 hr period. This can be compared with the constant value $\approx 5 \times 10^{-9} \text{ yr}^{-1}$ used by

Spruit & Ritter (1983) for all periods approaching and through the period gap.

3.2. Schematic Analysis of System Evolution

The magnetic complexity increase of the secondary star as the system spins up toward the 3.2 hr period is responsible for a decrease in angular-momentum-loss efficiency. We show here that the decrease happens to be large and fast enough to suppress mass accretion and explain the period gap, as predicted by Spruit & Ritter (1983), Rappaport et al. (1983), and Taam & Spruit (1989).

Following the approaches of Spruit & Ritter (1983) and Knigge et al. (2011), we model the evolution of a single system as it approaches the upper boundary of the period gap. We emphasize that the method used here is schematic and based on homologous stellar models calibrated with the Grossman et al. (1974) main sequence, and should ultimately be verified using more detailed stellar evolution models. Such validation of the Spruit & Ritter magnetic disruption mechanism for producing a period gap when using full stellar evolution models has recently been presented by Paxton et al. (2015), Kalomeni et al. (2016), and references therein. The difference in our study is that \dot{J}_{dip}/J does not change instantaneously, but still changes abruptly (much faster than the Kelvin–helmholtz timescale), by the same amplitude of $\approx 90\%$ as in Spruit & Ritter (1983), and near the upper boundary of the period gap. While this could potentially make a difference in a detailed stellar evolutionary model, the similarity in the angular-momentum-loss suppression and the fact that the homologous model results in detachment lends support for this proof-of-concept study.

We assume the secondary star has an initial mass of $M_2 = 0.42 M_\odot$ and an initial radius of $R_e \approx 0.9 M^{0.8}$, which is that expected from the mass–radius relation for a lower-main-sequence star in thermal equilibrium (Whyte & Eggleton 1980; Iben & Tutukov 1984; Knigge et al. 2011). If the accretion timescale ($\tau_{\dot{M}_2} = M_2/\dot{M}_2$, where \dot{M}_2 is the secondary’s mass-loss rate through accretion) is shorter than the thermal (Kelvin–Helmholtz) timescale of the donor star, $\tau_{\text{kh}} \sim GM^2/R$, then the secondary star is taken out of thermal equilibrium and inflates as a consequence of adiabatic mass loss. The mass–radius relation in the adiabatic limit becomes $R \propto M^{-1/3}$ (Rappaport et al. 1982), but CV donors turn out to be somewhere in between thermal equilibrium and the adiabatic limit when accreting fast enough. Theoretical expectations and observations suggest that in this regime $R \sim M^{0.65}$ (Patterson et al. 2005; Knigge 2006; Knigge et al. 2011). When approaching the minimum period (≈ 80 minutes), the angular momentum loss through gravitational radiation increases rapidly, further pushing the secondary star toward the adiabatic regime and, as a consequence, the mass–radius relationship becomes $R \sim M_2^{0.21}$ (Knigge et al. 2011). We use this relationship for systems with $M_2 < 0.1 M_\odot$ minutes.

We evolve the system for 10^9 years with a time step of 10^5 years. For each step we calculate the angular momentum loss using the equations above (CG18) with the complexity function discussed in Section 2. In addition, we include the angular momentum loss due to gravitational radiation given by Paczyński (1967b),

$$\dot{J}_{\text{GR}} = -\frac{32}{5} \frac{G^{7/2}}{c^5} \frac{M_1^2 M_2^2 M^{1/2}}{a^{7/2}}, \quad (4)$$

with G being the universal gravitational constant, $M = M_1 + M_2$, a the orbital separation, and c the speed of light. This contribution to the spin-up process becomes important for periods shorter than ~ 2 hr.

Whenever the donor star is in contact with the Roche lobe there is mass transfer. We compute the accretion rate using Knigge et al. (2011) and Equations (1)–(3) and assume $R \sim M^{0.65}$. If $\tau_{M_2} < \tau_{kh}$, the donor will detach from its Roche lobe and its radius will decrease at a rate $\dot{R}_2 \sim (R_2 - R_e)/\tau_{kh}$ toward thermal equilibrium. The thermal timescale of the reference donor star used by Spruit & Ritter (1983) above the period gap ($M = 0.28 M_\odot$, $R = 0.285 R_\odot$) is $\tau_{kh} \approx 3 \times 10^8$. We use this reference value to set the normalization factor for $\tau_{kh} \propto GM^2/R$. It might be argued that the actual timescale for the radius to adjust to a change in accretion rate is shorter than the equilibrium Kelvin–Helmholtz scale τ_{kh} (see, for example, Stehle et al. 1996; Knigge et al. 2011). In our evolutionary model we find the exact value of the radius shrinkage timescale is not critical for detachment, as long as the change in \dot{J} is fast enough to overcome the decrease in the orbital angular momentum so that the ratio J_{orb}/\dot{J} increases. This is satisfied in our model for both τ_{kh} and τ_{adj} ; \dot{J}/J decreases on a timescale of approximately 2×10^7 years, to be compared with a value of $\tau_{\text{adj}} \approx 8 \times 10^7$ years at a period of 3 hr (Knigge et al. 2011).

As the system evolves, the donor star is losing mass and becoming of a later spectral type. We account for this with a convective turnover time that evolves with the mass of the secondary star following Wright et al. (2011). However, our results do not change qualitatively when assuming a constant convective turnover time consistent with those expected for late M dwarfs (~ 100).

At each step, the orbital period follows from

$$P = 9\pi(2G)^{-1/2} \left(\frac{R_2^3}{M_2} \right)^{1/2} \quad (5)$$

(Paczynski & Sienkiewicz 1981; Spruit & Ritter 1983).

Figure 2 shows the angular-momentum-loss rate (top), the radius (middle), and the mass-loss rate (bottom) evolution of a single CV system with time. We find a fast but smooth decrease ($\sim 90\%$) in magnetic braking near the upper boundary of the period gap that allows the secondary star to return to thermal equilibrium. As a consequence, its radius (green line in the bottom panel) decreases, detaching from its Roche lobe (red line in the bottom panel) and mass accretion stops, as predicted by Spruit & Ritter (1983).

4. Population Synthesis

We then synthesize a population of CVs to compare with histograms of the frequency of observed CVs as a function of orbital period. We use the same prescription that we used for a single system and that accounts for the complexity of the magnetic field in the angular-momentum-loss efficiency. Our primordial binary systems follow the usual assumptions. We start from a zero-age CV (ZACV) population with a primary mass, M_1 , from the Miller & Scalo (1979) initial mass function,

$$M_1(x) = 0.19x[(1-x)^{3/4} + 0.032(1-x)^{1/4}]^{-1},$$

with masses in the range $0.8 < M_1 < 8 M_\odot$ (Howell et al. 2001), and a secondary mass from a probability distribution as in Abt & Levy (1978), Halbwegs (1987), and Howell et al. (2001), $f(q) = 5/4 q^{1/4}$, where $q = M_2/M_1$. In order to select

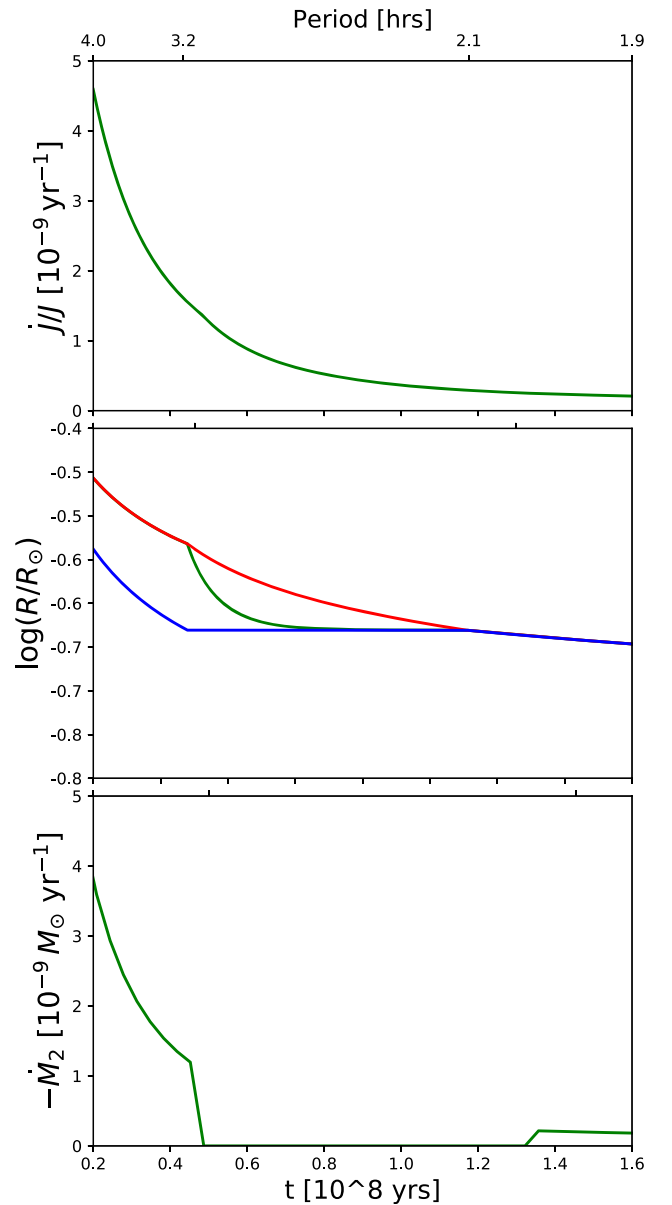


Figure 2. Single-system evolution of the relative angular momentum \dot{J}/J (top); the radius (green), the Roche lobe (red), and the equilibrium radius (blue) of the secondary star (middle); and the corresponding mass accretion \dot{M} (bottom). Note that because time increases toward the right and systems spin up, orbital period increases toward the left, contrary to how it is presented in Figure 1.

only systems that undergo a common-envelope phase we require that the radius of the Roche lobe of the primary be larger than the radius of a star of mass M_1 at the base of the giant branch (see, e.g., Paczyński 1967a; Webbink 1979, 1985, 1992; de Kool 1992; Howell et al. 2001 and references therein). We assume that a common-envelope phase occurs and that the duration of the spiral-in is sufficiently short (10^4 years; see references above) that the mass of the secondary does not change significantly during the episode (see, e.g., Taam et al. 1978; Miller & Scalo 1979; Livio & Soker 1988; Webbink 1992; Rappaport et al. 1994; Taam & Sandquist 1998). We then compute the final mass for the WD, $M_1 = M_{\text{core}}$, as in Howell et al. (2001).

Once we have generated the initial ZACVs masses, we compute the initial radius of the secondary assuming it is in thermal equilibrium, $R_2 = 0.9M^{0.8}$, as we did in Section 3. This is justified since CVs spend most of their time in this regime and, if magnetic braking is fast enough, the system will quickly transition to a different M_2 – R_2 regime. We then calculate their orbital period using Equation (5) as for the single-system evolution. Out of an initial population of $\sim 10^6$, we typically end up with 10^4 zero-age pre-CVs (consistent with Howell et al. 2000). We generate a new set of ZACVs every 10^5 years to account for a uniform rate of star formation.

We evolve these populations for 10^9 years and produce a histogram for the number of systems in each period bin (see the top panel of Figure 3). In addition, we make a histogram of the number of systems times their accretion luminosity, $L_{\text{acc}} \propto GM_1M_2/R_1$ (see, for example, Knigge et al. 2011 and references therein), which acts as a proxy for the observability for these systems (bottom panel of Figure 3). We find that as systems spin up they accumulate at shorter periods, reflecting the decreasing magnetic braking (see Figure 2). The brightness of systems at periods of approximately 3 hr drops sharply, and the period gap naturally arises from the magnetic disruption of angular-momentum-loss efficiency. They become visible again after they reach $P \approx 2$ hr, when spin-up rates increase again as a result of gravitational radiation becoming important.

The goal of this study is to show that stellar magnetic complexity evolution provides a natural explanation for the CV period gap while not requiring any change in the dynamo generation rate of magnetic flux, consistent with X-ray observations. Explaining the period distribution of systems below the period gap is out of the scope of this paper. It is in that spirit that we use a simplified model for the period bouncer decrease in the mass–radius relation at short periods (Knigge et al. 2011).

5. Conclusions

We have found that existing ZDI observations of late M dwarfs support a picture of increasing surface magnetic field complexity with decreasing rotation period for values of the period of several hours. This is consistent with the stellar spin-down model presented by CG18 that explains the bimodal rotation period distributions of stars in young open clusters in terms of evolving surface magnetic complexity. Greater magnetic complexity leads to suppression of mass loss and a shortening of the magnetic “lever” that acts as the rotational brake in late-type stars. Consequently, as CVs evolve toward shorter periods they experience a reduction in angular-momentum-loss rate and a reduction in the accretion rate driven by magnetic braking, as conjectured by Taam & Spruit (1989).

We have modeled a synthetic population of CVs using the standard CV evolution equations (Spruit & Ritter 1983; Knigge et al. 2011) together with the magnetic braking prescription provided in CG18. As periods approach 3.2 hr, the reduction in angular momentum loss is so rapid and efficient ($\sim 90\%$) that the accretion rate in most systems drops sufficiently to allow the puffed-up donor star to shrink back into thermal equilibrium. These are just the conditions that Spruit & Ritter (1983) pointed out would produce the CV period gap and that Taam & Spruit (1989) found could arise from an increase in surface magnetic complexity. The secondary star no longer fills its Roche lobe and mass accretion stops, rendering it

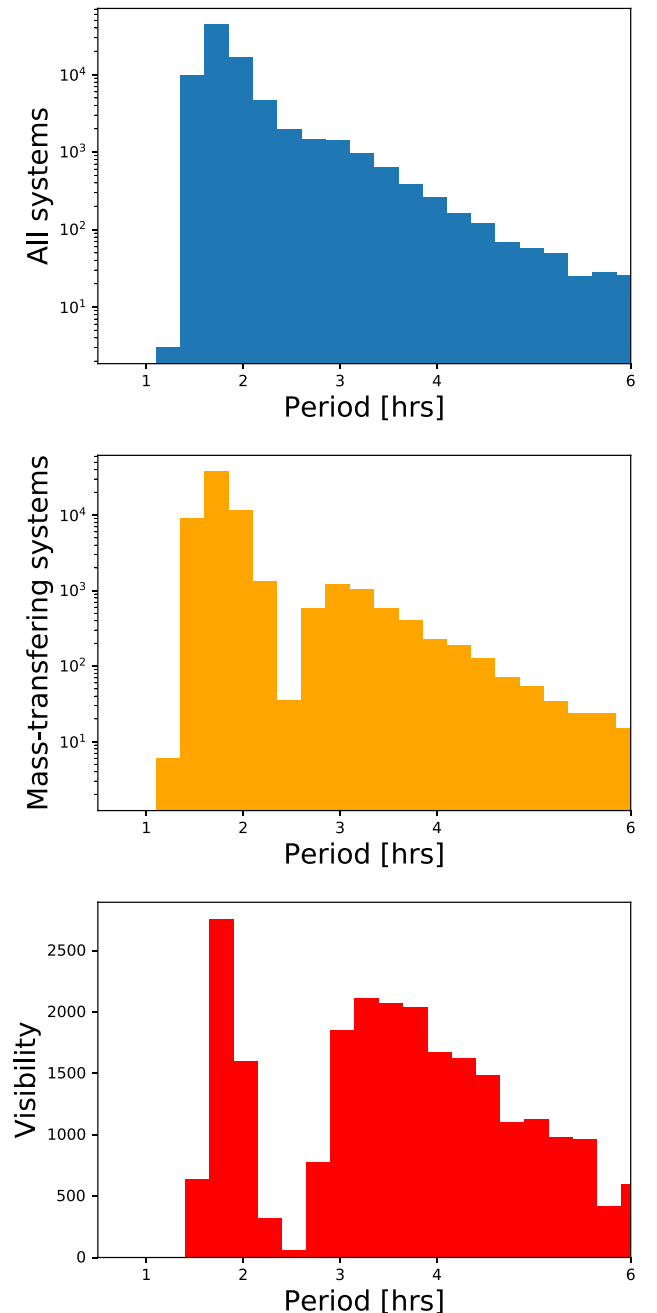


Figure 3. Histogram of expected number of systems (both accreting and not accreting) as a function of orbital periods (top), histogram of expected accreting systems (middle), and the sum of the accretion luminosity per bin in units of 10^{32} erg s^{-1} (bottom). We find that 38% of the systems lie above, 51% below, and 11% within the gap






observationally inconspicuous. However, the system continues to lose angular momentum through magnetic braking at this slower rate and eventually (at $P \approx 2$ hr) the orbital separation decreases enough for accretion to resume and consequently for the system to become conspicuous again. Our model predicts the presence of a few systems accreting within the gap, consistent with observations.

The explanation of the period gap in terms of an increase in magnetic complexity of the secondary as systems approach the gap as first suggested by Taam & Spruit (1989), rather than the dynamo itself shutting down, is fully consistent with X-ray

observations indicating that magnetic field generation is equally efficient above and below the M dwarf fully convective limit. The disrupted magnetic braking idea of Spruit & Ritter (1983) and Rappaport et al. (1983) is not broken.

We thank Rosanne Di Stefano, Christian Knigge, Gerrit Schellenberger, and Henk Spruit for useful comments and discussion and the referee for helpful suggestions. C.G. was supported by *Chandra* grant GO7-18017X, *XMM-Newton* grant 80NSSC18K0401, and *HST* grant GO-13754.0001-A during the course of this work. J.J.D. was supported by NASA contract NAS8-03060 to the *Chandra X-ray Center*. J.D.A.G. was supported by *Chandra* grants AR4-15000X and GO5-16021X. S.P.M. was supported by NASA Living with a Star grant number NNX16AC11G. O.C. was supported by NASA Astrobiology Institute grant NNX15AE05G. Simulation results were obtained using the Space Weather Modeling Framework, developed by the Center for Space Environment Modeling, at the University of Michigan with funding support from NASA ESS, NASA ESTO-CT, NSF KDI, and DoD MURI. Simulations were performed on NASA's PLEIADES cluster under award SMD-16-6857.

ORCID iDs

C. Garraffo  <https://orcid.org/0000-0002-8791-6286>
 J. J. Drake  <https://orcid.org/0000-0002-0210-2276>
 J. D. Alvarado-Gomez  <https://orcid.org/0000-0001-5052-3473>
 S. P. Moschou  <https://orcid.org/0000-0002-2470-2109>
 O. Cohen  <https://orcid.org/0000-0003-3721-0215>

References

- Abt, H. A., & Levy, S. G. 1978, *ApJS*, **36**, 241
 Alvarado-Gómez, J. D., Hussain, G. A. J., Grunhut, J., et al. 2015, *A&A*, **582**, A38
 de Kool, M. 1992, *A&A*, **261**, 188
 Donati, J.-F. 2003, in *EAS Publ. Ser. 9, Magnetism and Activity of the Sun and Stars*, ed. J. Arnaud & N. Meunier (Les Ulis: EDP Sciences), 169
 Donati, J.-F., & Brown, S. F. 1997, *A&A*, **326**, 1135
 Donati, J.-F., & Landstreet, J. D. 2009, *ARA&A*, **47**, 333
 Eggleton, P., Mitton, S., & Whelan, J. (ed.) 1976, *IAU Symp. 73, Structure and Evolution of Close Binary Systems* (Dordrecht: D. Reidel)
 Faulkner, J. 1971, *ApJL*, **170**, L99
 Finley, A. J., Matt, S. P., & See, V. 2018, *ApJ*, **864**, 125
 Garraffo, C., Cohen, O., Drake, J. J., & Downs, C. 2013, *ApJ*, **764**, 32
 Garraffo, C., Drake, J. J., & Cohen, O. 2015, *ApJ*, **813**, 40
 Garraffo, C., Drake, J. J., & Cohen, O. 2016, *A&A*, **595**, A110
 Garraffo, C., Drake, J. J., Dotter, A., et al. 2018, *ApJ*, **862**, 90
 Grossman, A. S., Hays, D., & Graboske, H. C., Jr. 1974, *A&A*, **30**, 95
 Halbwachs, J. L. 1987, *A&A*, **183**, 234
 Howell, S. B., Ciardi, D. R., Dhillon, V. S., & Skidmore, W. 2000, *ApJ*, **530**, 904
 Howell, S. B., Nelson, L. A., & Rappaport, S. 2001, *ApJ*, **550**, 897
 Hussain, G. A. J., Donati, J.-F., Collier Cameron, A., & Barnes, J. R. 2000, *MNRAS*, **318**, 961
 Iben, I., Jr., & Tutukov, A. V. 1984, *ApJ*, **284**, 719
 Kalomeni, B., Nelson, L., Rappaport, S., et al. 2016, *ApJ*, **833**, 83
 Knigge, C. 2006, *MNRAS*, **373**, 484
 Knigge, C., Baraffe, I., & Patterson, J. 2011, *ApJS*, **194**, 28
 Livio, M., & Shaviv, G. 1983, *Cataclysmic Variables and Related Objects* (Dordrecht: D. Reidel)
 Livio, M., & Soker, N. 1988, *ApJ*, **329**, 764
 Marsden, S. C., Jardine, M. M., Ramírez Vélez, J. C., et al. 2011, *MNRAS*, **413**, 1922
 Miller, G. E., & Scalo, J. M. 1979, *ApJS*, **41**, 513
 Morin, J., Donati, J.-F., Petit, P., et al. 2010, *MNRAS*, **407**, 2269
 Paczyński, B. 1967a, *AcA*, **17**, 193
 Paczyński, B. 1967b, *AcA*, **17**, 287
 Paczynski, B., & Sienkiewicz, R. 1981, *ApJL*, **248**, L27
 Patterson, J., Kemp, J., Harvey, D. A., et al. 2005, *PASP*, **117**, 1204
 Paxton, B., Marchant, P., Schwab, J., et al. 2015, *ApJS*, **220**, 15
 Pevtsov, A. A., Fisher, G. H., Acton, L. W., et al. 2003, *ApJ*, **598**, 1387
 Rappaport, S., Di Stefano, R., & Smith, J. D. 1994, *ApJ*, **426**, 692
 Rappaport, S., Joss, P. C., & Webbink, R. F. 1982, *ApJ*, **254**, 616
 Rappaport, S., Verbunt, F., & Joss, P. C. 1983, *ApJ*, **275**, 713
 Réville, V., Brun, A. S., Matt, S. P., Strugarek, A., & Pinto, R. F. 2015, *ApJ*, **798**, 116
 Ritter, H. 1984, *A&AS*, **57**, 385
 Robinson, E. L., Barker, E. S., Cochran, A. L., Cochran, W. D., & Nather, R. E. 1981, *ApJ*, **251**, 611
 Spruit, H. C. 2011, in *The Sun, the Solar Wind, and the Heliosphere*, ed. M. P. Miralles & J. Sánchez Almeida (Berlin: Springer), 39
 Spruit, H. C., & Ritter, H. 1983, *A&A*, **124**, 267
 Stehle, R., Ritter, H., & Kolb, U. 1996, *MNRAS*, **279**, 581
 Taam, R. E., Bodenheimer, P., & Ostriker, J. P. 1978, *ApJ*, **222**, 269
 Taam, R. E., & Sandquist, E. 1998, in *ASP Conf. Ser. 138, 1997 Pacific Rim Conf. on Stellar Astrophysics*, ed. K. L. Chan, K. S. Cheng, & H. P. Singh (San Francisco, CA: ASP), 349
 Taam, R. E., & Spruit, H. C. 1989, *ApJ*, **345**, 972
 Verbunt, F., & Zwaan, C. 1981, *A&A*, **100**, L7
 Waite, I. A., Marsden, S. C., Carter, B. D., et al. 2011, *MNRAS*, **413**, 1949
 Waite, I. A., Marsden, S. C., Carter, B. D., et al. 2015, *MNRAS*, **449**, 8
 Webbink, R. F. 1979, *ApJ*, **227**, 178
 Webbink, R. F. 1985, in *Stellar Evolution and Binaries*, ed. J. E. Pringle & R. A. Wade (Dordrecht: D. Reidel), 39
 Webbink, R. F. 1992, in *X-Ray Binaries and the Formation of Binary and Millisecond Radio Pulsars* (Dordrecht: Springer), 269
 Whyte, C. A., & Eggleton, P. P. 1980, *MNRAS*, **190**, 801
 Wright, N. J., & Drake, J. J. 2016, *Natur*, **535**, 526
 Wright, N. J., Drake, J. J., Mamajek, E. E., & Henry, G. W. 2011, *ApJ*, **743**, 48